Photogrammetric Record, 17(99): 419–439 (April 2002)

THROUGH-WATER CLOSE RANGE DIGITAL PHOTOGRAMMETRY IN FLUME AND FIELD ENVIRONMENTS

JUSTIN B. BUTLER
E-Giving, London

STUART N. LANE (s.lane@geography.leeds.ac.uk)
University of Leeds

JIM H. CHANDLER (j.h.chandler@lboro.ac.uk)
Loughborough University

EKATERINI PORFIRI
University of Bath

(Based on a paper read at the Thompson Symposium of the Photogrammetric Society held at the University of Surrey on 9th April 2000)

Abstract

Measurement of the structure of gravel-bed river surfaces is crucial for understanding both bed roughness and the sediment entrainment process. This paper describes the use of close range digital photogrammetry to measure and monitor change occurring in submerged river gravel-beds in both flume and field environments. High-resolution digital elevation models (DEMs) were obtained and two-media (through air and water) techniques were used to correct for the effects of refraction at the air/water interface. Although suitable refractive models have been developed, the use of proprietary software to generate DEMs automatically introduces the problem of how to re-establish collinearity. A simple refraction correction algorithm based upon analytical geometry was developed and is described. This algorithm was designed for use after initial DEM acquisition and allows any photogrammetric software package to be used for data acquisition. Application of this algorithm led to improvements in DEM accuracy by reducing the systematic, depth-dependent bias caused by refraction.

Research carried out in a flume environment allowed the algorithm to be tested by measuring a flooded and drained bed surface. Non-systematic differences between the ''dry'' and ''wet'' DEMs arose from reductions in stereomatching success in the two-media case. This effect was thought to be due to light attenuation and the introduction of residual parallax. Results suggest that close range digital photogrammetry can be used to extract high

quality DEMs of submerged topography in both flume and field fluvial environments, which represents a particularly exciting development for fluvial geomorphologists.

KEYWORDS: bedform, flow modelling, fluvial geomorphology, two-media photogrammetry

INTRODUCTION

RECENT RESEARCH within the field of fluvial geomorphology has suggested that better specification of surface topography is crucial for the understanding of both the effects of roughness upon flow processes (Lane et al., 1998) and of roughness elements upon sediment entrainment and transport (Clifford et al., 1992; Hassan and Reid, 1990). The viability of close range digital photogrammetry for extracting high resolution DEMs of exposed gravel river-bed surfaces in the field has already been confirmed (Butler et al., 1998), and these DEMs have been used to quantify the roughness properties of these surfaces (Butler et al., 2001). However, the fluvial geomorphologist is especially interested in water-submerged zones. Two-media photogrammetry represents a possible solution, at least for shallow and clear water situations. Through-water photogrammetry is a specific case of two-media photogrammetry, where the camera is above the water surface (in air) and the target is in a different medium (water). Despite a number of complicating factors, through-water photogrammetry has been used for mapping subaqueous topography using some form of elevated or airborne platform to support the cameras (Fryer, 1983; Westaway et al., 2001). These projects have adopted a correction for the effects of refraction at the air/water interface. With the development and application of digital photogrammetry, additional uncertainty remains over the inclusion of water on the performance of stereomatching algorithms.

Following on from these issues, the main aims of the research described in this paper are to:

(i) develop a methodology for extracting DEMs of river-bed gravels automatically using digital photogrammetry applied to imagery of submerged zones in laboratory flumes and the field;
(ii) investigate the effects of the presence of water on automated stereomatching by comparing stereomatched DEMs extracted from laboratory flume data, with and without the inclusion of water; and
(iii) to develop a fully-automated correction procedure to compensate for the effects of refraction at the air/water interface.

THEORY AND CONCEPTS OF TWO-MEDIA PHOTOGRAMMETRY

The basis of two-media photogrammetry has been widely addressed (Tewinkel, 1963; Shmutter and Bonfiglioli, 1967; Masry, 1974; Karara, 1972; Slama, 1980; Shan, 1994) and basic optical principles suggest that accurate through-water photogrammetry is theoretically possible. The main problem is that if the systematic error caused by refraction at the air/water interface is ignored, then derived or

apparent elevations are corrupted by a real/apparent depth effect. The geometry of the problem is shown in Fig. 1. For simplicity, and as with other studies, this research assumes that the water surface is planar.

Rays of light originating from an underwater point P are refracted at the planar air/water interface at P_A and P_B, prior to arriving and being recorded in the images exposed at camera stations A and B. If the systematic error is ignored, then the two lines AP_A and BP_B intersect approximately (but not exactly) at P'', the apparent depth of the point. The exact location of this point will depend on the position and orientation of the exposure stations. Without some form of correction, refraction acts to produce an image of the surface which appears to lie above (that is, at a shallower depth than) the real surface, and the original light rays are clearly not modelled by the collinearity condition. Light rays passing through the air/water interface are refracted according to Snell's law:

$$\frac{\sin r}{\sin i} = \frac{h}{h_A} = n \tag{1}$$

where i is the angle of incidence of a light ray originating from point P below the water surface, r is the angle of the refracted ray above the water surface, h is the actual water depth, h_A is the apparent water depth and n is the refractive index, a

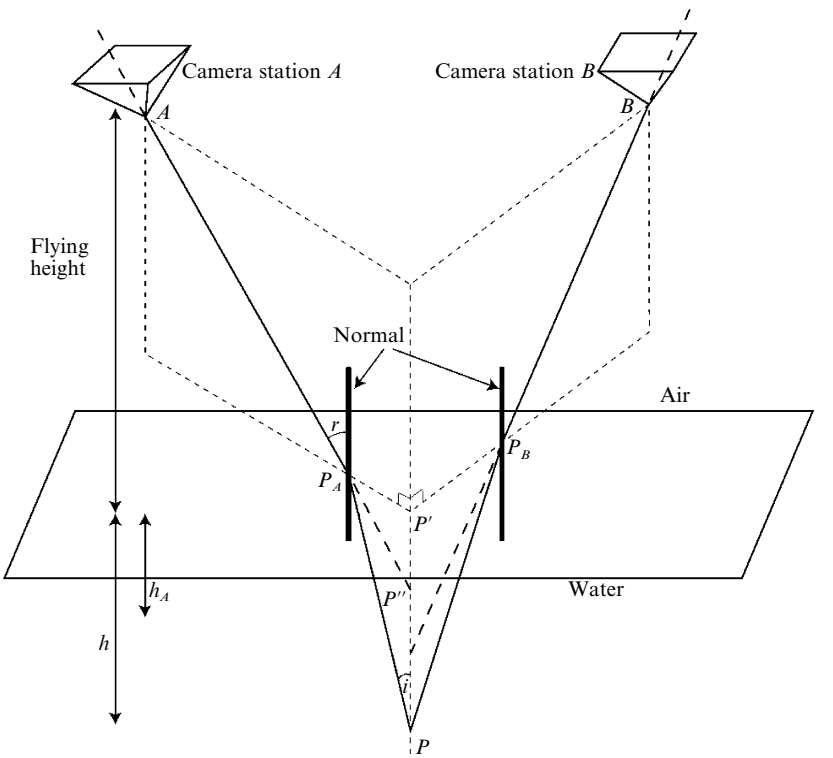

FIG. 1. Geometry of two-media photogrammetry (Fryer and Kniest, 1985).

value dependent on the optical properties of the two media (Fryer and Kniest, 1985). With regard to clear water, n has been shown to take a value of 1·340 and to vary by less than 1% ($\pm$0·007) for a wide range of temperature and salinity conditions (Jerlov, 1976). Application of (1) to h_A for each point re-validates the assumption of a perspective projection for that point (Fryer and Kniest, 1985).

There are, however, additional practical problems that need to be overcome. First, the position of the water surface must either be known or modelled mathematically (Rinner, 1969; Kniest, 1990). Second, the magnitude of the required correction (see Appendix) depends on the angle of incidence (i) (Fryer and Kniest, 1985), and the magnitude of the required correction increases with radial distance from the perspective centre of the camera lens. Finally, when using small-scale aerial photography as part of a photogrammetric survey, other effects such as water surface disturbance, differences between the imaging of water surface features on each frame due to the time lag between exposures, and turbid water may be important (Westaway et al., 2001). If the aim is to reconstruct submerged topography by using through-water photogrammetry, then simple application of (1) is insufficient to compensate for the refraction effect.

Conventional approaches developed to counteract refractive effects have involved the adjustment of image coordinates during the block adjustment phase (Rinner, 1969; Harris and Umbach, 1972; Newton, 1989). This procedure has required the computation of radial distortions in the image due to refraction, to reduce the bundle of incident rays to conformity with the perspective projection. The obvious disadvantage with this approach is that it requires modification of the block bundle adjustment, which is not easy to achieve with most commercially available software packages. Thus, in the course of this research, a refraction correction was developed that could be applied after the block adjustment phase and the automated extraction of a regular grid-based DEM.

METHODOLOGY

Refraction Correction Algorithm

Two alternative methods for refraction correction were considered: adjustment of the object (X, Y, Z) co-ordinates for each DEM point; and adjustment (reduction) of individual vertical (Z) values to compensate for refraction at each X, Y location. The first option is similar to the conventional formulation of the refractive model except that corrections are applied to the object space planimetric coordinates of derived DEMs, as opposed to the image space coordinates of refracted points. However, alteration of the planimetric coordinates of DEM points would require subsequent re-sampling to reconstruct the original regular grid. Some form of interpolation would be required, such as using a bilinear or cubic convolution, and selection would introduce added uncertainty into the procedure. By modifying the Z coordinate only, the second method automatically retains the grid-based structure of the DEMs, and was chosen for initial development and experimentation. It was felt that if this proved to be inappropriate or of insufficient accuracy, then the other, more sophisticated, approach would be considered. The model used in this study is based upon three dimensional analytical geometry and the theory used for its development is provided in the Appendix.

In order to avoid any modification to the block bundle adjustment, all photocontrol points are assumed to lie above the water surface, typically in the form of small targets located on the surface of the perspex sheet used to flatten the water surface. Due to the use of only a thin layer (3 mm) of perspex, the refraction correction model assumes also that the air/perspex/water interface can be simplified to just air/water, an approach adopted and recommended by many authors (Fryer, 1983; Newton, 1989). The model also assumes that the interface is both planar and horizontal, which in the case of a floating perspex basin is acceptable.

APPLICATION AND TESTING

The refraction correction model was subjected to a series of exhaustive tests carried out using imagery acquired in a laboratory flume. The approach was also developed and applied in a natural river channel in Scotland.

Data Acquisition

For the laboratory case, a tilting flume (8 m long and 0·3 m wide, with transparent sidewalls) located in the Department of Geography, University of Cambridge was used to acquire stereophotography from an exposed, simulated gravel riverbed. The gravels were water-worked for several hours until a stable bed with a realistic structure was obtained (depth = approximately 10 cm; Reynolds number = 150 000; Froude number = 1·51). A constant source of illumination was provided by fluorescent strip lighting. The selection of long exposures obviated the need for flash photography.

A transparent perspex sheet (3 mm thick) was used to flatten the water surface at the time of exposure and five photogrammetric targets were fixed on the upper surface of the perspex. Two semi-metric Hasselblad ELX cameras, supported on a specially designed movable gantry, were used to acquire 1:15 scale panchromatic stereophotographs (Fig. 2). The cameras were mounted 1·2 m above the bed and were separated by 310 mm. Such geometry provided approximately 65% overlap between the images, with a base:distance ratio of approximately 1:4, which met general accuracy requirements (height estimation to within ± 1 to 2 mm). The use of three exposure stations provided continuous coverage of a 1 m strip of exposed flumebed. The approximate principal distance of the cameras was 80 mm; the exact value of this parameter and an appropriate lens model was determined using self-calibrating bundle adjustment methods.

The flume was then flooded to depths of 12 cm followed by 25 cm, with care being taken that surface disturbance was kept to a minimum. Similar exposure stations were also used to acquire one-medium (though-air) photography, to allow DEMs representing the flumebed to be compared with and without water. The accuracy of the refractive models could then be assessed directly. All the photographs were scanned at 20 μm with 256 shades of grey, using a Helava DSW 100 scanning workstation.

Permanent control points, at fixed positions within the hydraulics laboratory, were used to establish the coordinates of a series of photocontrol targets using two total stations and an intersection method. Some of the targets were located on the surface of the horizontal perspex sheet, and allowed the elevation of the sheet to

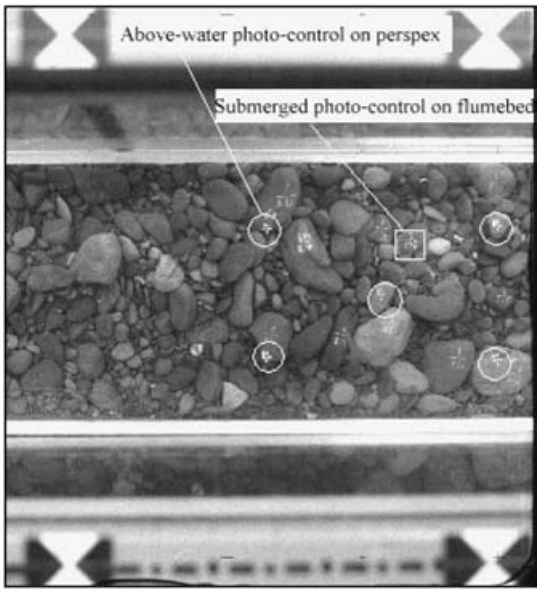

FIG. 2. Example of an image taken of the tilting flume in the Department of Geography, University of Cambridge.

be estimated for each water depth. A total of 26 additional photo-control targets were placed upon the flumebed itself; these were used to assess the success of the block bundle adjustment in the two-media case.

For the real river study, data was acquired from a reach of the River Affric, Scotland (Ordnance Survey grid reference: NH 128204). This is a typical upland, coarse-grained river, within which a number of large gravel bars become exposed at low flow. The Hasselblad cameras were supported approximately 2·2 m above the water surface by a floating tetrahedron. A purpose-built box with a clear, non-reflective perspex base ($1{\cdot}5 \times 1{\cdot}5 \times 0{\cdot}003$ m) was floated on the water surface directly beneath the cameras to create a horizontal, planar air/water interface. Photography was acquired after midday and with the sun low enough to minimise reflection from the perspex sheet, using the same Hasselblad cameras used for the flume study. The water depth was approximately 0·2 m and so the camera-to-object distance was approximately 2·4 m. The two cameras were separated by 0·35 m, providing approximately 60% forward overlap and a base:distance ratio of about 1:7.

Five photogrammetric targets were glued onto the surface of the perspex box to provide above-water photocontrol. Survey measurements were made to these points using a total station, and were subsequently used to estimate object space coordinates and accuracies for all targets within the predetermined local coordinate system. Negatives were scanned at 20 μm to produce digital imagery, where each pixel represented an area of approximately $0{\cdot}8 \times 0{\cdot}8$ mm in the object space. This set-up was capable of generating a DEM at a ground resolution of 3 mm, in line with study requirements.

Photogrammetric Data Processing

Automated DEM extraction was performed using the OrthoMAX module of ERDAS Imagine software (see Butler et al. (1998) for full coverage). The internal geometry of the Hasselblad cameras was established using results from an offline self-calibrating bundle adjustment. The rmse associated with the affine transformation used for interior orientation was approximately 3 μm for imagery of the exposed and submerged bed.

In the flume case, the targets on the perspex sheet were clearly visible in the photography taken using the shallower water depth (12 cm). These targets were measured on the images and were used as constrained control points within OrthoMAX to estimate the exterior orientation of the cameras. Because refraction at the air/water interface meant that targeted points on the bed surface did not fulfil the condition of collinearity, these were (re)classified as unconstrained tie points to assess the impact of refraction on the height estimates.

For imagery acquired using the greater depth (25 cm), despite attempts to maximise the depth of field at the time of exposure, the targets on the Perspex sheet remained blurred. As it was not possible to repeat the acquisition of two-media photography, the blurred targets meant that above-water surface control was not available in this case. Although in violation of the condition of collinearity, the bed surface points, which were clearly visible through the water, were used to provide photocontrol. This non-rigorous approach was expected to generate large error residuals on the exterior orientation (EO) parameters due to the ignored effects of refraction. However, it was felt that this approximate approach might still provide useful height estimates in the absence of surface control. These two approaches are hereafter referred to as Method 1 (using surface points) and Method 2 (using bed points). Although unnecessary due to the availability of surface control, a DEM was also collected using Method 2 but using imagery taken using the shallower water depth. This DEM enabled additional results, pertaining to the performance of Method 2, to be obtained.

Photogrammetric data processing for the field application was carried out in a similar manner to that for the flume application, this time using the estimated coordinates of the targets on the perspex box as photocontrol.

DEM Extraction

The ERDAS automated DEM extraction software was employed to derive the surface DEMs; it uses the normalised cross-correlation method and orthorectified image patches to identify homologous points in the overlapping images (ERDAS, 1995). The algorithm does require appropriate specification of strategy parameters, which is an issue of more general concern (Smith et al., 1997; Gooch et al., 1999; Butler et al., 1998). Consequently, the DEMs were collected using both a default and an "optimum" parameter set. The latter was identified using the methodology outlined in Butler et al. (1998). It was considered that the y parallax parameter, which controls the vertical search range, would play a critical role in improving the success of matching in the two-media case. This is because the introduction of residual parallax due to refraction may impede the extent to which searches along the epipolar line are successful. It was expected that improvements in matching

success were most likely to occur at the margins of the image overlap, where distortions due to refraction are greatest. Thus, one image pair from the flume case was used to check this. The y parallax parameter was perturbed over a range of values, with DEMs collected for each, whilst remaining collection parameters were kept at their default values. DEMs were all collected using the highest possible grid spacing, as defined by the image scale: 1·5 mm in the flume case and 3 mm in the field case. This density produced DEMs with about 133 000 elevations in the flume case (for an area that is $1{\cdot}0 \times 0{\cdot}3$ m and based upon 3 stereopairs) and with about 40 000 elevations in the field case (for an area that is $0{\cdot}60 \times 0{\cdot}60$ m and based on a single stereopair).

DEM Quality Assessment

The DEM quality assessment procedure outlined in Butler et al. (1998) was applied to the flume and field data. As part of the qualitative and semi-quantitative components of this procedure, ortho-imagery was generated, and DEM correlation statistics (which measure the percentage of matched points relative to the percentage of interpolated points) were recorded for each collected DEM. For the flume application, comparison of the stereomatching performance for the one- and two-media cases allowed the effects of water and perturbation of the y parallax parameter to be assessed. For quantitative DEM assessment, independent check points were used to compute accuracy statistics from ''wet'' DEMs before and after the refraction correction had been applied. This procedure enabled the performance of the refraction correction algorithm to be judged with reference to the quality of the derived data. The internal reliability of two-media photogrammetric measurement was also assessed by comparing one- and two-media DEMs, and was achieved on a point-by-point basis for corresponding areas. For the field data, acquisition of control points on the submerged bed was not possible due to constant disturbances caused by the flow and hence absolute DEM accuracy could not be assessed.

RESULTS

Qualitative Assessment of DEM Quality

Photogrammetrically acquired DEMs for the flume case, with a dry bed, at various water depths, and with optimised parameters are shown in Fig. 3. These DEMs suggest that the introduction of water results in only a minor reduction in the quality of topographic representation. Failure of the stereomatching algorithm towards the edges of each ''wet'' DEM is thought to be due to significant levels of residual parallax at the margins of the stereomodel due to refraction, which reduces the performance of stereomatching in these areas.

The use of the ''optimum'' parameter set does not appear to alter the visual appearance of the DEM significantly (Fig. 3(d)), although some clasts do appear to be better defined following collection parameter variation.

Photogrammetrically acquired DEMs of the submerged riverbed are illustrated in Fig. 4, where (a) shows the full area DEM and (b) shows a sub-area DEM, both of which were collected from a through-water stereopair. The brightest patches, which represent the highest elevations, correspond to the above-water photocontrol targets on the perspex surface. The pattern of grey values in Fig. 4(a) shows a

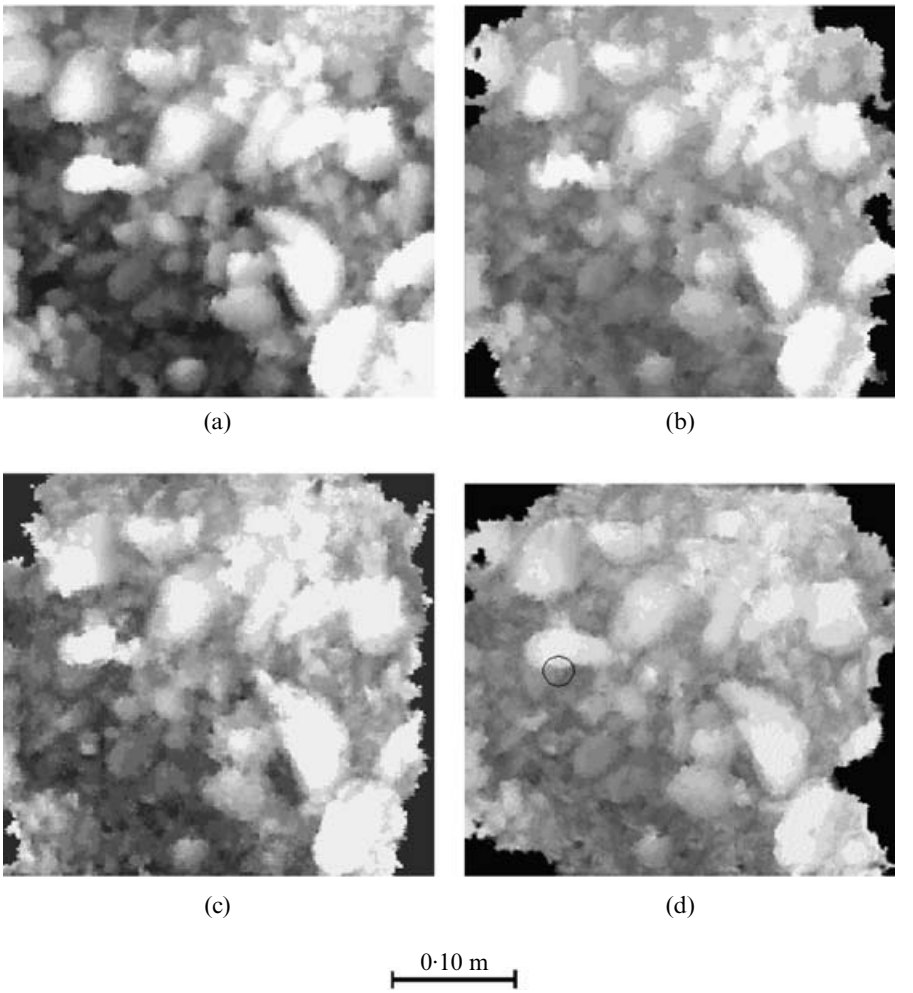

FIG. 3. DEMs of the flume obtained from data extracted: (a) through air; (b) through 12 cm of water; (c) through 25 cm of water; and (d) the same as (b) but using varied collection parameters. The circle in (d) shows an area where collection parameter variation has improved the topographic representation.

progression from shallow (approximately 10 cm) to deeper (approximately 25 cm) water from left to right, towards the centre of the channel. This gradient is also apparent in the sub-area DEM (Fig. 4(b)), in which individual clasts are seen to be clearly represented. Although there seems to be a relatively good topographic representation across the area of interest, shadows and reflections cast by the structural members of the tetrahedron onto the surface of the perspex were seen to cause failure of the matching algorithm in these areas. This effect provided an explanation for the linear features visible on the left-hand side of Fig. 4(a).

These qualitative results are encouraging, suggesting that field application of through-water digital photogrammetry is possible.

Stereomatching Results

Table I demonstrates the internal correlation statistics, estimated by the OrthoMAX software, for the wet DEMs derived from the flume case shown in Fig. 4. The addition of water reduced the level of "good" matches by 3·9% with a water depth of 12 cm, and 4·6% with a depth of 25 cm. The percentage of "poor" pixels was seen to decrease by approximately 9% following the addition of water, although this was accompanied by an increase in the percentage of "interpolated" pixels by almost 12%, irrespective of water depth. Somewhat better matching statistics were obtained for the field case (Table I), suggesting that introduction of water exerted less of a control upon matching performance than conventional controls (such as illumination and surface texture).

Refraction Correction Effects

Fig. 5 quantifies the spatial corrections computed by the refractive model for the field DEM. A range of positive height differences can be seen varying from approximately 1 mm to 70 mm, with larger corrections being applied in deeper areas

TABLE I. Effect of including water on collection results for the flume DEM.

Status category	*Flume: dry*	*Flume: 12 cm deep*	*Flume: 25 cm deep*	*Field*
Good (%)	9·1	5·1	4·5	11·8
Fair (%)	35·1	36·2	36·7	41·6
Poor (%)	22·2	13·3	13·7	20·2
Interpolated (%)	33·6	45·4	45·2	26·4

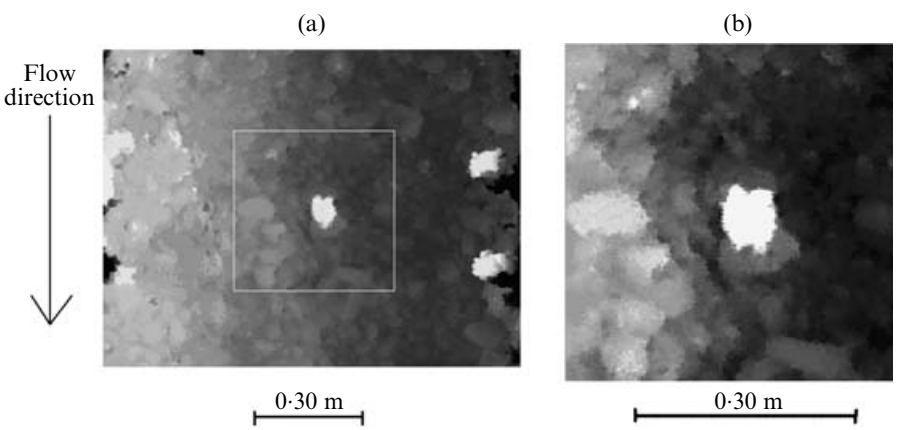

FIG. 4. DEMs acquired from the submerged riverbed data: (a) full area; (b) sub-area. The location of (b) within (a) is shown. These DEMs were collected using the default collection parameters.

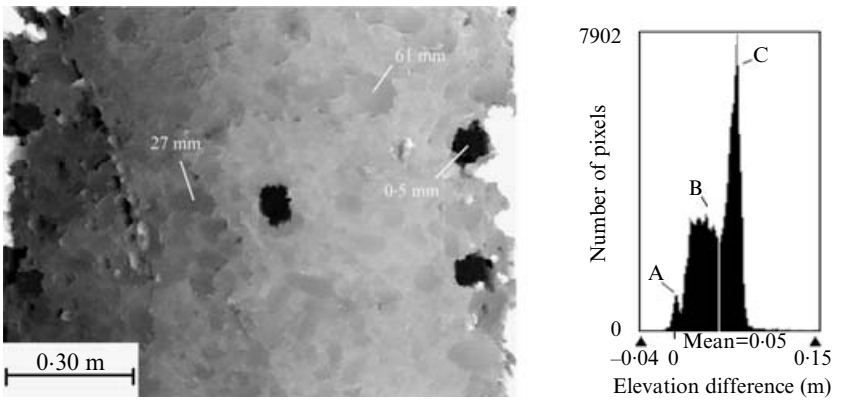

FIG. 5. (a) DEM of difference showing the spatial variation of elevation differences between the raw and refraction corrected field DEMs (elevation differences at various locations are marked on the image); (b) histogram of elevation differences calculated from (a).

towards the right-hand side of Fig. 5(a). As expected, shallower points on the tops of larger clasts generated smaller corrections than neighbouring deeper points, which fell in crevices between clasts. The histogram of depth corrections shows a multi-modal distribution with a mean of approximately 0·05 m (Fig. 5(b)). This suggests that although point elevations for the corrected DEM were, on average, approximately 0·05 m below those for the raw DEM, corrections were grouped into three size categories. Mode A in Fig. 5(b) was found to correspond to the smallest (sub-mm) corrections applied to points on the above-water photogrammetric targets. Intermediate corrections, represented by Mode B in Fig. 5(b), corresponded to points in the left-hand (shallower) side of the field DEM. Finally, Mode C, which represents the largest corrections, was found to be associated with deeper points in the right-hand side of Fig. 5(b). The tail of very large corrections in Fig. 5(b) corresponded to marginal areas of the DEM (shown in white in Fig. 5(a)) which contained erroneous pixel elevations caused by stereomatching failure. These results confirm the depth dependence of the correction algorithm and show that the refraction correction varies spatially. Most importantly, the test demonstrates the significance of an appropriate correction, even if only relative height estimates are required (for example, for a roughness statistic). Even simple roughness measures, like the local standard deviation of the surface, will be underestimated if an appropriate correction for refraction is not used.

Quantitative DEM Assessment using Independent Check Data

Fig. 6(a) presents the results of comparing independent check-point elevations and the nearest corresponding points before and after applying the refraction correction algorithm. These results relate to the submerged DEM that was acquired using through-water imagery applied to a depth of 12 cm, with above-water surface control on the perspex sheet. As Fig. 6(a) shows, the mean unsigned error (MUE) associated with the two-media DEM prior to refraction correction registered a

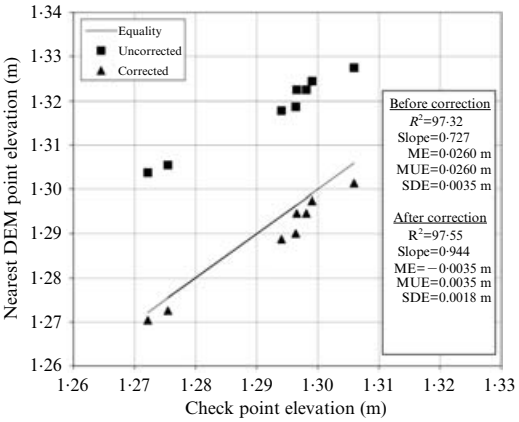
Equality
Uncorrected
Corrected
Before correction
R^2=97·32
Slope=0·727
ME=0·0260 m
MUE=0·0260 m
SDE=0·0035 m
After correction
R^2=97·55
Slope=0·944
ME=−0·0035 m
MUE=0.0035 m
SDE=0.0018 m
Nearest DEM point elevation (m)
Check point elevation (m)
1·26
1·27
1·28
1·29
1·30
1·31
1·32
1·33
1·34

(a)

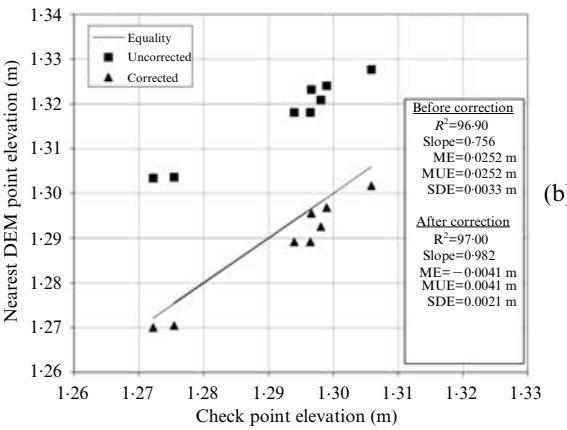
Equality
Uncorrected
Corrected
Before correction
R^2=96·90
Slope=0·756
ME=0·0252 m
MUE=0·0252 m
SDE=0·0033 m
After correction
R^2=97·00
Slope=0·982
ME=−0·0041 m
MUE=0.0041 m
SDE=0.0021 m
Nearest DEM point elevation (m)
Check point elevation (m)
1·26
1·27
1·28
1·29
1·30
1·31
1·32
1·33
1·34

(b)

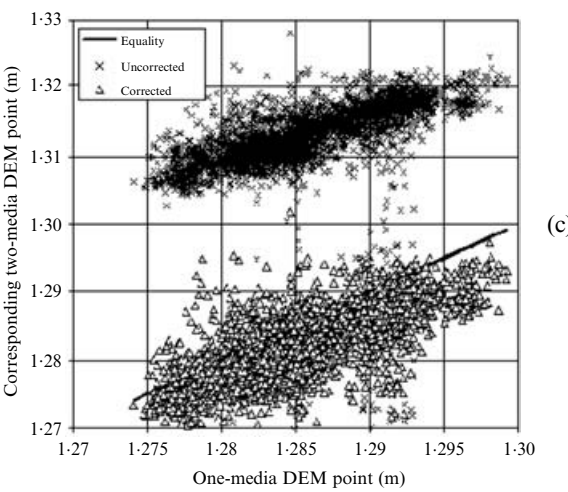
Equality
Uncorrected
Corrected
Corresponding two-media DEM point (m)
One-media DEM point (m)
1·27
1·275
1·28
1·285
1·29
1·295
1·30
1·31
1·32
1·33

(c)

FIG. 6. (a) Elevation cross-plot showing ground control point elevation versus the nearest corresponding DEM point for a DEM obtained from data extracted through 12 cm of water using default collection parameters; (b) as for (a) but using varied correction parameters (results pre- and post-refraction correction are shown); (c) scatter plot showing elevations in the raw and refraction-corrected two-media DEMs relative to corresponding elevations in the one-medium DEM. [R^2 = % of variance in checkpoint elevations; ME = mean error; MUE = mean unsigned error; SDE = standard deviation of error.]

large (approximately 0·026 m) datum shift relative to the check-point elevations on the bed. Refraction correction reduced the datum discrepancy between the one- and two-media cases (MUE = 0·0035 m). A slight overcompensation for the refractive effect is suggested by the negative value of mean error (ME) for the corrected DEM, although the magnitude of this shift (approximately −0·0035 m) was small relative to the total height range of the surface. More importantly, by providing a measure of global precision, the standard deviation of error (SDE) for pre- and post-corrected DEMs was seen to decrease from 0·0035 m to 0·0018 m, which represented a 49% improvement in precision following correction. The significant (density $\rho < 0{\cdot}05$) increase in the slope of the regression line, towards a value of unity, also suggested that greater height errors at lower elevations (that is, greater depths) received larger corrections. This finding provided evidence that the correction algorithm compensates for the depth-dependence of the real/apparent depth effect. Fig. 6(b) shows that collecting the DEM using the "optimum" parameter set did not significantly alter the accuracy statistics ($\rho < 0{\cdot}05$) or the results from applying the refraction correction algorithm.

Internal Reliability Tests

The number of data points shown in Fig. 6(a) is small relative to the number of pixels in the DEM and Lane et al. (2000) demonstrated that this could result in erroneous conclusions about controls upon DEM quality. One way to avoid this is to undertake internal reliability tests. This was possible for the flume case because the dry dataset was available. Fig. 6(c) compares raw and corrected elevations relative to the one-medium DEM for the uncorrected and corrected case. This shows a desired reduction in the raw elevation values following refraction correction, which produces a surface that does not contain a datum shift. Some evidence of over-correction at higher elevations (lower depths) is seen towards the right of Fig. 6(c), although this may have been due to the effects of a reduction in sample size.

DISCUSSION

A Successful Approach?

The strategy adopted for generating accurate DEMs through water clearly relied upon the standard DEM extraction procedure being successful in the two-media case. Initially, it was feared that refraction of the light rays due to the water/perspex/air interface would cause the cross-correlation procedure to fail, thereby preventing use of this simplified approach. It is clear that these initial fears were unfounded and that DEMs were successfully generated, including those from

water depths up to 0·25 m and with a camera elevation of only 1·2 m, which is a ratio of 20% of the camera height. It would appear that although the original light rays do not fulfil collinearity per se, the apparent rays actually do so. This effect occurs because the light rays are refracted in the same plane as their original path and is, of course, the reason why it is possible to perceive an apparent surface in a stereomodel. This result is clearly significant because it means that any proprietary DEM extraction software can be used to create the original "apparent" DEM surface, which can then be corrected later using an offline program. It is now appropriate to assess the validity of the refraction correction algorithm developed, both qualitatively and quantitatively.

Quality of Through-water DEMs

In qualitative terms, the topographic representations afforded by through-water DEMs extracted from field and flume data appear to be comparable and of good quality. This conclusion was suggested by the visual inspection of DEMs, which showed that individual clasts were well defined in each case. DEM quality was lower towards DEM edges in both applications, and it is suspected that this is due to residual y parallax. Although increasing the y parallax parameter was found to improve matching success in marginal areas, this was also accompanied by a reduction in the overall level of matching success. As such, variation of this parameter is not considered to be beneficial for optimising surface quality.

Stereomatching failure in the vicinity of DEM edges meant that a continuous strip of elevation data could not be generated. It is therefore recommended that the endlap between successive images should be increased in cases where continuous coverage is required. Despite these edge effects, matching success within the central portion of each DEM was acceptable, and this was higher in the case of the field DEMs (Table I) relative to that for DEMs extracted from the flume data. Differences in overall matching success between the two applications are probably influenced by levels of image contrast, and this is supported by comparing the signal-to-noise ratios (SNRs) calculated from imagery of the flumebed (approximately 2·0) with that from the field (approximately 2·4). The higher SNR of the field imagery may have been due to the better, natural illumination, relative to that which was possible using artificial lighting in the laboratory. As the inclusion of water acts to attenuate illumination at the bed, especially at greater depths, this might explain the increase (11·5%) in the level of interpolation that resulted from submerging the flumebed, relative to the one-medium case.

Variation of collection parameters prior to DEM collection can be used to:

(i) reduce the level of interpolation (Table I);
(ii) improve the precision of individual matches; and
(iii) in some cases, improve the definition of individual grain boundaries (for example, Fig. 3(d)).

With regard to (iii), this improvement is perhaps caused by a reduction in the smoothing effect that results from interpolation. However, it must be reiterated that an improvement in matching success may not lead to more accurate DEM points (Butler et al., 1998). Tests showed that collection parameter variation does not significantly improve accuracy statistics in the two-media case (Fig. 6(b)). Once

again, this may be a bona fide result, although it is more likely that changes in DEM accuracy in the vicinity of crevasses were not being detected, due to the lack of check points in these areas.

Accuracy of Through-water DEMs

The results from the flume application are summarised in Table II. These can be used to evaluate: (i) the effects of refraction upon DEM accuracy; and (ii) the relative performance of the two methods used to establish exterior orientation.

Table II shows that refraction at the air/water interface resulted in a positive systematic error as reflected in the value of MUE for the uncorrected DEM collected using Method 1 where surface photo-control was located on the perspex. When using control on the bed (Method 2), the datum shift caused by refraction was only apparent in the corrected DEM (Table II). As expected, the value of this error was seen to be less at a depth of 12 cm (MUE = 0·0392 m, using Method 2) than at 25 cm (MUE = 0·0726 m, using Method 2). This result confirmed that the magnitude of the real/apparent depth effect was depth dependent.

Comparison with the one-medium case shows that refraction:

(i) decreases DEM quality (measured by SDE in Table II), and introduces errors into the elevations by an amount that is proportional to depth; and
(ii) reduces the slope of the regression line through the scatter of points in Figs. 6(a) and 6(c).

TABLE II. Summary of results for the flume tests for two-media DEM quality assessment showing the effect of refraction correction upon various measures of DEM quality.

Level of correction/ application	*Adjusted* $R^{2\dagger}$	*Slope*	*Mean error (m)*	*Mean unsigned error (m)*	*Standard deviation of error (m)*	*% points matched*	*% points inter-polated*
Uncorrected							
1-medium*	97·96	0·963	0·0000	0·0011	0·0015	67·0	33·0
2-media (12 cm)[a]	97·32	0·727	0·0256	0·0256	0·0035	54·9	45·1
2-media (12 cm)[b]	96·42	0·873	−0·0017	0·0019	0·0024	54·7	45·3
2-media (25cm)[b]	98·60	0·800	0·0008	0·0020	0·0017	54·8	45·2
Corrected							
2-media (12 cm)[a]	97·55	0·944	−0·0035[†]	0·0035[†]	0·0018[†]	54·9	45·1
2-media (12 cm)[b]	96·74	1·128	−0·0392	0·0392	0·0027	54·7	45·3
2-media (25cm)[b]	98·79	1·031	−0·0726	0·0726	0·0013	54·8	45·2
Corrected/optimised collection parameters							
2-media (12 cm)[b]	97·00	0·982	−0·0041[†]	0·0041[†]	0·0021[†]	74·3	25·7

R^2 is the % of variance in check-point elevations explained by the photogrammetrically-derived elevations.
*Results from "dry" DEM are shown for comparison.
[a]Results for through-water DEMs extracted using above-water surface control (Method 1).
[b]Results for through-water DEMs extracted using control on the bed (Method 2).
[†]Values are not significantly different at the 95% level.

With regard to (i), this effect does not appear to become more severe at greater depths, although the smaller than expected value of SDE in Table II for the uncorrected DEM at 25 cm depth (0·0017 m) may be due to the method of DEM extraction, which was based on the use of control on the bed. As far as (ii) is concerned, this effect further suggests that at lower elevations (greater depths) the errors caused by refraction are greater.

As Table II shows, the magnitude of the datum shift caused by refraction was lower when Method 1 was used (MUE = 0·0256 m; 12 cm depth), compared to that from using Method 2 (MUE = 0·0392 m; 12 cm depth). This result occurs because, in the first case (Method 1), the real/apparent depth effect was being measured directly using accurately estimated camera heights. In the case of Method 2, greater uncertainty in the estimation of camera heights may have caused the systematic error due to refraction to be overestimated. It is interesting to note that the residual for the partially constrained camera elevation was roughly equal to the discrepancy between the two estimates of the datum shift.

When photocontrol points were positioned on the perspex (Method 1) and the refraction correction model was used, the global accuracy of the DEM (MUE) decreased from 0·0256 to 0·0035 m and the SDE decreased from ±0·0035 to ±0·0018 m (the latter being equivalent to ±0·13% of the camera-to-object distance). The refraction correction removed the systematic datum shift caused by the real/apparent depth effect and improved the precision of corrected points, when judged relative to the check data. These results were particularly encouraging and suggested vertical accuracies that improve upon those from previous through-water research using analytical photogrammetry. For example, Fryer (1984) found that the standard deviation of depth measurements, using submerged levelling staves as targets, was ±0·2% of the camera-to-object distance. Further, as Fryer (1984) found that vertical accuracy was independent of water depth between 0·3 m and 1·3 m, it is expected that these results may hold good for DEMs extracted using greater water depths, to the point where the SNR of the imagery begins to decrease significantly. These accuracies were appropriate for the overall project needs and it was considered unnecessary to develop the model further.

When using photocontrol points beneath the perspex (Method 2), which are uncorrected for refraction, it is clear that these DEMs must still be corrected for the real/apparent depth effect. This correction can be achieved by: (i) applying the refraction correction algorithm; and (ii) removing the datum shift which results from under-estimation of the camera heights.

In summary, as the bottom row of Table II demonstrates, the highest quality two-media DEM is obtained by using surface mounted photo-control points, an optimised set of strategy parameters and the simple refractive model provided in the Appendix.

CONCLUSIONS

The aims of this research were to assess the potential of digital photogrammetry for collecting high-resolution DEMs of submerged topography, and to develop and apply a correction procedure to reduce the errors introduced by the presence of water. The results show that it is possible to use standard proprietary digital photogrammetric software for obtaining high quality, small scale topo-

graphic information from submerged zones in both a laboratory flume and a natural gravel-bed river. The effects of refraction can then be reduced by applying a simple refraction correction algorithm that corrects each DEM point for the real/apparent depth effect, without the need for resampling.

Apparatus for acquiring close range, through-water photography can be constructed inexpensively, and the use of anti-reflective perspex sheeting, to flatten the water surface and provide surface control, greatly simplifies the two-media problem. The direct use of underwater control is not a rigorous approach to the two-media problem, but can be used to provide acceptable results if above-water surface control is unavailable.

ACKNOWLEDGEMENTS

This research was funded by a NERC studentship awarded to J. B. Butler and an EPSRC Grant awarded to S. N. Lane, J. H. Chandler and K. S. Richards. J. Hooker (City University) and A. Hayes (Cambridge University) designed and constructed the field apparatus.

REFERENCES

BUTLER, J. B., LANE, S. N. and CHANDLER, J. H., 1998. Assessment of DEM quality for characterizing surface roughness using close range digital photogrammetry. *Photogrammetric Record*, 16(92): 271–291.

BUTLER, J. B., LANE, S. N. and CHANDLER, J. H., 2001. Application of two-dimensional fractal analysis to the characterisation of gravel-bed river surface structure. *Mathematical Geology*, 33(3): 301–330.

CLIFFORD, N. J., ROBERT, A. and RICHARDS, K. S., 1992. Estimation of flow resistance in gravel-bedded rivers: a physical explanation of the multiplier of roughness length. *Earth Surface Processes and Landforms*, 17(2): 111–126.

ERDAS, 1995. *ERDAS Imagine Version 8.2.* ERDAS Inc., Atlanta. 121 pages.

FRYER, J. G., 1983. Photogrammetry through shallow water. *Australian Journal of Geodesy, Photogrammetry and Surveying*, 38: 25–38.

FRYER, J. G., 1984. Errors in depths determined by through-water photogrammetry. *Ibid.,* 40: 29–39.

FRYER, J. G. and KNIEST, H. K., 1985. Some strategies for improving the accuracy of depths determined by through-water photogrammetry. *Ibid.,* 43: 45–60.

GOOCH, M. J., CHANDLER, J. H. and STOJIC, M., 1999. Accuracy assessment of digital elevation models generated using the Erdas Imagine OrthoMAX digital photogrammetric system. *Photogrammetric Record,* 16(93): 519–531.

HARRIS, W. D. and UMBACH, M. J., 1972. Underwater mapping. *Photogrammetric Engineering*, 38(8): 765–772.

HASSAN, M. A. and REID, I., 1990. The influence of microform bed roughness elements on flow and sediment transport in gravel bed rivers. *Earth Surface Processes and Landforms*, 15(8): 739–750.

JERLOV, N. G., 1976. *Marine Optics.* Elsevier, Amsterdam. 231 pages.

KARARA, H. M., 1972. Simple cameras for close-range applications. *Photogrammetric Engineering*, 38(5): 447–451.

KNIEST, H. T., 1990. *Photogrammetry through an air-water interface*. University of Newcastle, New South Wales, Research Report No. 055.11.1990. 185 pages.

LANE, S. N., RICHARDS, K. S. and CHANDLER, J. H. (Eds.), 1998. *Landform Monitoring, Modelling and Analysis.* Wiley, Chichester. 454 pages.

LANE, S. N., JAMES, T. D. and CROWELL, M. D., 2000. Application of digital photogrammetry to complex topography for geomorphological research. *Photogrammetric Record,* 16(95): 793–821.

MASRY, S. E., 1974. Digital correlation principles, *Photogrammetric Engineering*, 40(3): 303–308.
NEWTON, I., 1989. Underwater photogrammetry. Chapter 11 in *Non-topographic Photogrammetry* (Ed. H. M. Karara). American Society for Photogrammetry and Remote Sensing, Falls Church, Virginia. 445 pages: 147–166.
RINNER, K., 1969. Problems of two-media photogrammetry. *Photogrammetric Engineering*, 35(3): 275–282.
SHAN, J., 1994. Relative orientation for two-media photogrammetry. *Photogrammetric Record*, 14(84): 993–999.
SHMUTTER, B. and BONFIGLIOLI, L., 1967. Orientation problems in two-medium photogrammetry. *Photogrammetric Engineering*, 33(12): 1421–1428.
SLAMA, C. C. (Editor-in-Chief), 1980. *Manual of Photogrammetry*. Fourth edition. American Society of Photogrammetry, Falls Church, Virginia. 1056 pages.
SMITH, M. J., SMITH, D. G. and TRAGHEIM, D. G., 1997. DEMs and ortho-images from aerial photographs. *Photogrammetric Record*, 15(90): 945–950.
TEWINKEL, G. C., 1963. Water depths from aerial photographs. *Photogrammetric Engineering*, 29(6): 1037–1042.
WESTAWAY, R. M., LANE, S. N. and HICKS, D. M., 2001. Remote sensing of clear-water, shallow, gravel-bed rivers using digital photogrametry. *Photogrammetric Engineering & Remote Sensing*, 67(11): 1271–1281.

APPENDIX

It is assumed that the air/water interface, OP_1, shown in Fig. A1, is horizontal and planar. A ray of light originating from point P (X_P, Y_P, Z_P) is refracted at the air/water interface at P_1 (X_{P_1}, Y_{P_1}, Z_{P_1}) and is recorded in the image taken at camera station S_1 (X_{S_1}, Y_{S_1}, Z_{S_1}). The apparent object space position of P is A (X_A, Y_A, Z_A). Given estimates for (X_{S_1}, Y_{S_1}, Z_{S_1}), a value for Z_{P_1} and the apparent object space co-ordinates (X_A, Y_A, Z_A) of each DEM point, a correction, h_C, to the apparent depth, h_A, to obtain the real depth, h, can be computed using equations (A7), (A10), (A6) and (A12).

From Snell's law (1):

$$i = \sin^{-1}\left(\frac{\sin r}{n}\right) \tag{A1}$$

where i = angle of incidence, r = angle of refraction and n = refractive index.

From Fig. A1,

$$h_A = x/\tan r \tag{A2}$$

$$h = x/\tan i \tag{A3}$$

where x is the separation of P_1 and P in the x direction.

Thus,

$$h = \frac{h_A \tan r}{\tan i}. \tag{A4}$$

Substituting (A1) into (A4) and simplifying gives

$$h = \frac{h_A \tan r}{\tan\left(\sin^{-1}\left(\frac{\sin r}{n}\right)\right)} \tag{A5}$$

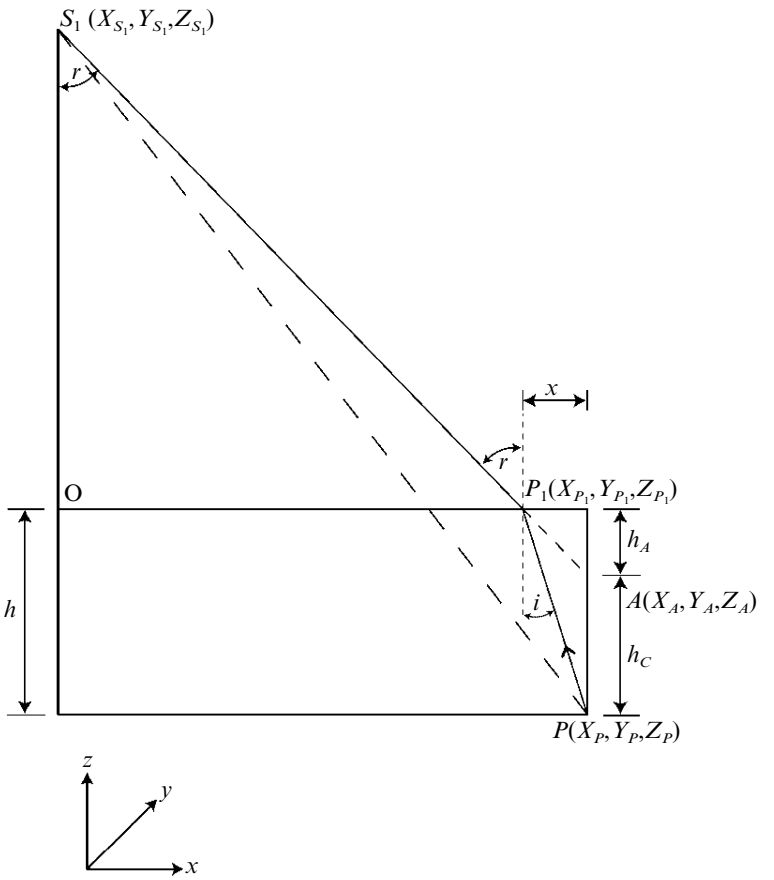

FIG. A1. A method for refraction correction based on analytical geometry.

which, for all realistic values of r, approximates to

$$h \cong \frac{h_A \tan r}{\tan\left(\frac{r}{n}\right)}. \tag{A6}$$

Although angle r is not known, it can be computed in three dimensions using direction ratios $(X_A - X_{S_1};\ Y_A - Y_{S_1};\ Z_A - Z_{S_1})$, and the distance (D) between the camera station to the initial (uncorrected) point:

$$D = \sqrt{(X_A - X_{S_1})^2 + (Y_A - Y_{S_1})^2 + (Z_A - Z_{S_1})^2}. \tag{A7}$$

The direction cosines from the camera to the initial point are given by

$$\frac{X_A - X_{S_1}}{D};\ \frac{Y_A - Y_{S_1}}{D};\ \frac{Z_A - Z_{S_1}}{D}. \tag{A8}$$

The angle σ between two lines with direction cosines l_1, m_1, n_1 and l_2, m_2, n_2 is given by:

$$\cos\sigma = l_1 l_2 + m_1 m_2 + n_1 n_2. \tag{A9}$$

The direction cosines of the normal to a horizontal plane are $(0, 0, -1)$, and so the angle σ in (A9) is equivalent to angle r and simplifies to

$$r = \cos^{-1}\left[-\left(\frac{Z_A - Z_{S_1}}{D} \right) \right]. \tag{A10}$$

As the apparent depth is given by

$$h_A = Z_{P_1} - Z_A, \tag{A11}$$

r from (A10) can then be substituted into (A6) to give the real depth, h. The depth correction, h_C, can be finally calculated using

$$h_C = h - h_A. \tag{A12}$$

This procedure can be carried out for both the left-hand and right-hand cameras to obtain two estimates for h_C. The average of both corrections is used to determine a corrected elevation at each DEM point.

Résumé

La détermination de la structure de surface des graviers au fond des fleuves est essentielle pour une bonne compréhension de la rugosité du lit et du processus d'entraînement des sédiments. On présente dans cet article une application de la photogrammétrie numérique rapprochée pour déterminer et suivre les variations qui interviennent sur les graviers dans le lit des cours d'eau, tant dans des canaux d'amenée que sur le terrain. On a obtenu des modèles numériques des altitudes (MNA) à haute résolution en corrigeant les effets de la réfraction à la surface de séparation des deux milieux (air/eau). Bien que les modèles de réfraction dont on dispose soient bien adaptés, se pose le problème du rétablissement de la colinéarité dans la conception des logiciels générant automatiquement le MNA. Aussi a t-on développé un algorithme simple de correction de la réfraction, en s'appuyant sur la géométrie analytique. On présente cet algorithme qui doit être utilisé une fois acquis le MNA initial, ce qui permet de recourir ensuite à n'importe quel jeu de logiciels photogrammétriques pour la saisie des données. On améliore ainsi la précision du MNA par la réduction du biais de réfraction dépendant systématiquement de la profondeur sous l'eau. On a pu tester cet algorithme sur un canal d'amenée et déterminer la surface du lit lors d'une inondation et après évacuation de l'eau. Les différences que l'on a trouvées entre l'état à sec et en eau du MNA ne sont pas apparues systématiques; on pense qu'elles sont dues à une atténuation de la lumière dans l'eau et à l'apparition d'une parallaxe résiduelle et non à un biais de réfraction. Ces résultats montrent que l'on peut utiliser la photogrammétrie rapprochée pour établir des MNA de très bonne qualité et déterminer la topographie sous le niveau de

l'eau dans les canaux d'amenée comme dans les fleuves, sur le terrain. Cela constitue une application qui devrait tout à fait intéresser les géomorphologues spécialisés dans les cours d'eau.

Zusammenfassung

Die Vermessung der Struktur von Kiesbettoberflächen in Flüssen ist wichtig für das Verständnis der Flussbettrauhigkeit und des Sedimenttransportes. Dieser Beitrag behandelt den Einsatz digitaler Nahbereichsphotogrammetrie zur Messung und Verfolgung der Änderungen, die im überfluteten Kiesbett von Flüssen auftreten, wobei hier sowohl Schwemmrinnen als auch natürliche Umgebungen betrachtet werden. Es wurden hochauflösende Digitale Höhenmodelle (DHM) generiert und Zweimedientechniken (Luft/Wasser) wurden eingesetzt, um die Brechungseffekte an der Schnittstelle Luft/Wasser zu korrigieren. Obwohl geeignete Refraktionsmodelle entwickelt worden sind, wirft der Einsatz eigener Software zur automatischen DHM Generierung das Problem auf, die Kollinearitätsbedingung wiederherzustellen. Deshalb wurde ein einfacher Algorithmus zur Korrektur der Refraktion auf der Basis analytischer Geometrie entwickelt, der hier beschrieben wird. Das Verfahren wurde so gestaltet, dass es nach einer initialen DHM Erfassung eingesetzt wird, womit jedes photogrammetrische Softwarepaket für die Datenerfassung genutzt werden kann. Durch die Anwendung dieses Algorithmus wurde die DHM Genauigkeit verbessert, dadurch dass der systematische, tiefenabhängige Bias, verursacht durch die Refraktion, verringert wird. Untersuchungen in einer Schwemmrinnen Umgebung ermöglichten es, den Algorithmus in einem überfluteten und einem entwässerten Flussbett zu testen. Nicht systematische Differenzen zwischen dem ''trockenen'' und dem ''nassen'' DHM stammten von der geringeren Erfolgsrate bei der Stereobildzuordnung im Zweimedienfall. Es wurde angenommen, dass dieser Effekt durch Lichtabfall und der Einführung von Restparallaxen entstand. Die Ergebnisse deuten darauf hin, dass digitale Nahbereichsphotogrammetrie verwendet werden kann, um hochgenaue DHMs von überfluteter Topographie in Schwemmrinnen und natürlichen Flussumgebungen zu erfassen, was sicherlich eine richtungsweisende Entwicklung für Flussgeomorphologen bedeutet.